

AD-A039 491

DAVID W TAYLOR NAVAL SHIP RESEARCH AND DEVELOPMENT CE--ETC F/G 20/4
COMPUTATION OF THE VELOCITY POTENTIAL FOR A PULSATING SOURCE IN--ETC(U)
DEC 75 D J SHERIDAN

UNCLASSIFIED

SPD-652-01

NL

1 of 1
AD
A039491

[Frame 1: Diagram]	[Frame 2: Diagram]	[Frame 3: Diagram]	[Frame 4: Diagram]	[Frame 5: Diagram]	[Frame 6: Diagram]	[Frame 7: Diagram]	[Frame 8: Diagram]	[Frame 9: Diagram]	[Frame 10: Diagram]	[Frame 11: Diagram]	[Frame 12: Diagram]
[Frame 13: Diagram]	[Frame 14: Diagram]	[Frame 15: Diagram]	[Frame 16: Diagram]	[Frame 17: Diagram]	[Frame 18: Diagram]	[Frame 19: Diagram]	[Frame 20: Diagram]	[Frame 21: Diagram]	[Frame 22: Diagram]	[Frame 23: Diagram]	[Frame 24: Diagram]
[Frame 25: Diagram]	[Frame 26: Diagram]	[Frame 27: Diagram]	[Frame 28: Diagram]	[Frame 29: Diagram]	[Frame 30: Diagram]	[Frame 31: Diagram]	[Frame 32: Diagram]	[Frame 33: Diagram]	[Frame 34: Diagram]	[Frame 35: Diagram]	[Frame 36: END DATE FILMED 6-77]

Report SPD-652-01

COMPUTATION OF THE VELOCITY POTENTIAL FOR A PULSATING SOURCE IN A FLUID WITH FREE SURFACE AND FINITE DEPTH

DDC No.

DDC FILE COPY.

ADA 039491

DAVID W. TAYLOR
NAVAL SHIP RESEARCH AND DEVELOPMENT CENTER

Bethesda, Maryland 20084



12

[Handwritten signature]

COMPUTATION OF THE VELOCITY POTENTIAL FOR A
PULSATING SOURCE IN A FLUID WITH FREE SURFACE
AND FINITE DEPTH

by

D. J. Sheridan

DDC
MAY 16 1977
NAVY
[Handwritten initials]

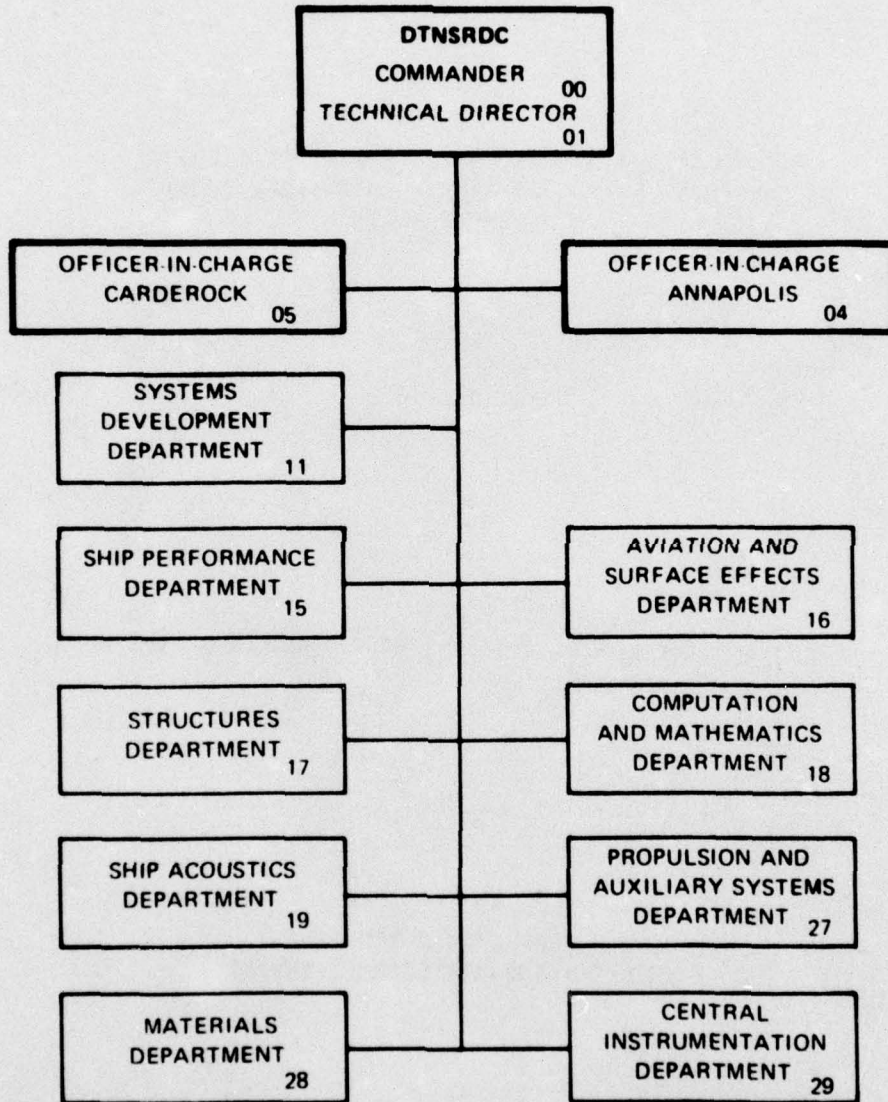
Approved for public release; distribution unlimited

SHIP PERFORMANCE DEPARTMENT
RESEARCH AND DEVELOPMENT REPORT

December 1975

Report SPD 652-01

MAJOR DTNSRDC ORGANIZATIONAL COMPONENTS



UNCLASSIFIED

SECURITY CLASSIFICATION OF THIS PAGE (When Data Entered)

REPORT DOCUMENTATION PAGE		READ INSTRUCTIONS BEFORE COMPLETING FORM
1. REPORT NUMBER SPD-652-01	2. GOVT ACCESSION NO.	3. RECIPIENT'S CATALOG NUMBER
4. TITLE (and Subtitle) Computation of the Velocity Potential for a Pulsating Source in a Fluid with Free Surface and Finite Depth	5. TYPE OF REPORT & PERIOD COVERED Final (Departmental) Rept. Log	6. PERFORMING ORG. REPORT NUMBER
7. AUTHOR(s) D. J. Sheridan	8. CONTRACT OR GRANT NUMBER(s)	
9. PERFORMING ORGANIZATION NAME AND ADDRESS David W. Taylor Naval Ship R&D Center Bethesda, Maryland 20084	10. PROGRAM ELEMENT PROJECT TASK AREA & WORK UNIT NUMBERS Program Element 61153N Proj. No. SR02301 - Task Area SR0230101	
11. CONTROLLING OFFICE NAME AND ADDRESS	12. REPORT DATE December 1975	
14. MONITORING AGENCY NAME & ADDRESS (if different from Controlling Office) Naval Sea Systems Command Washington, DC 20362	13. NUMBER OF PAGES 47	15. SECURITY CLASS. (of this report) Unclassified
16. DISTRIBUTION STATEMENT (of this Report) Approved for Public Release: Distribution Unlimited		15a. DECLASSIFICATION/DOWNGRADING SCHEDULE
17. DISTRIBUTION STATEMENT (of the abstract entered in Block 20, if different from Report)		
18. SUPPLEMENTARY NOTES		
19. KEY WORDS (Continue on reverse side if necessary and identify by block number) Oscillating Source Hydrodynamics Free Surface Finite Depth		
20. ABSTRACT (Continue on reverse side if necessary and identify by block number) A technique is presented that allows the numerical evaluation of the velocity potential for a pulsating source in a fluid with a free surface and finite depth. The series expansion used to obtain a numerically tractable representation of the finite depth potential is in a form suitable for use with ship motion programs that employ source distribution techniques in conjunction with strip theory. The effects of water depth, source submergence, and		

DDC
FORM 1
MAY 16 1977
C

389 694

DD FORM 1473
1 JAN 73

EDITION OF 1 NOV 65 IS OBSOLETE
S/N 0102-014-6601

UNCLASSIFIED

SECURITY CLASSIFICATION OF THIS PAGE (When Data Entered)

UNCLASSIFIED

SECURITY CLASSIFICATION OF THIS PAGE(When Data Entered)

20. (Continued)

pulsating frequency on the free-surface elevation are explored with the intent of demonstrating finite depth effects on readily identifiable physical parameter.

UNCLASSIFIED

TABLE OF CONTENTS

	<u>PAGE</u>
ABSTRACT	1
ADMINISTRATIVE INFORMATION	1
INTRODUCTION	2
FORMULATION OF THE PROBLEM	6
SOLUTION OF THE PROBLEM	9
PRESENTATION AND DISCUSSION OF RESULTS	10
CONCLUSIONS	18
ACKNOWLEDGMENTS	19
BIBLIOGRAPHY AND REFERENCES	20
APPENDIX A DERIVATION OF THE VELOCITY POTENTIAL FOR WATER OF FINITE DEPTH	23
APPENDIX B SERIES EXPANSION USED TO NUMERICALLY EVALUATE THE VELOCITY POTENTIAL	34
APPENDIX C COMPUTER PROGRAM, LISTING, SAMPLE INPUT AND SAMPLE OUTPUT	37

SESSION for	
RTIS	White Section <input checked="" type="checkbox"/>
FIG	Buff Section <input type="checkbox"/>
UNANNOUNCED	<input type="checkbox"/>
JUSTIFICATION	<input type="checkbox"/>
BY	
DISTRIBUTION/AVAILABILITY CODES	
Dist.	AVAIL. AND/OR SPECIAL
A	

LIST OF FIGURES

		<u>PAGE</u>
Figure 1	Reference Coordinate System and Problem Geometry	6
Figure 2	Comparison of Wave Form from the Finite and Infinite Depth Potentials	13
Figure 3	The Effects of Varying Source Submergence	14
Figure 4	The Effects of Varying Water Depth	16
Figure 5	Lower Frequency Wave Forms	17
Figure A.1	Coordinate System and Problem Geometry for Derivation of the Potential Expression	23
Figure A.2	Contour of Integration	28
Figure C.1	Summation Term versus the Number of Terms in the Sum for the $x=a=0$ Case	40
Figure C.2	Representative Graphical Solutions for the Equation: $n \tanh n = B$	40
Figure C.3	Representative Graphical Solution for the Equation: $s \tan s = -B$	40

ABSTRACT

A technique is presented that allows the numerical evaluation of the velocity potential for a pulsating source in a fluid with a free surface and finite depth. The series expansion used to obtain a numerically tractable representation of the finite depth potential is in a form suitable for use with ship motion programs that employ source distribution techniques in conjunction with strip theory. The effects of water depth, source submergence, and pulsating frequency on the free-surface elevation are explored with the intent of demonstrating finite depth effects on a readily identifiable physical parameter.

ADMINISTRATIVE INFORMATION

The study described herein evolved from research supported by the Naval Ship Systems Command (NAVSHIPS) under the General Hydromechanics Research Program of the Naval Ship Research and Development Center (NSRDC). Funding was provided under Subproject S-R02301, Task 0101.

INTRODUCTION

One of the most useful techniques employed in the theoretical analysis of ship motions is the "strip theory" approach, originally derived for pitch and heave motions by Korvin-Kroukovsky and W.R. Jacobs (1957) and later improved and extended by Salvesen, Tuck, and Faltinsen (1970). This theory is based on the assumption that the three-dimensional hydrodynamic properties of a ship may be expressed as the sum of the two-dimensional characteristics of specified transverse cross sections of the ship hull. Strip theory has proved to be a useful tool for analytic ship motion analysis and enjoys wide application. Since the use of the theory requires that the two-dimensional hydrodynamic characteristics of various cross-sections be determined, techniques designed to provide this information form an important role for proper application of strip theory to ship motion work. The two principal means of obtaining these properties are the multipole expansion method (often referred to as the conformal mapping technique) and the source distribution method.

The multipole expansion technique was first employed by Ursell (1949) for determining the hydrodynamic characteristics of a circular cylinder oscillating in the free surface. Several investigators have contributed to the extension of this technique to the Lewis forms and later to more general shapes; especially notable are the works of Grimm (1953) and Porter (1960). Korvin-Kroukovsky (1957), Gerritsma (1966), Smith (1966), Grim (1960), and Vassilopoulos (1964) all employed the multipole expansion technique to determine the two-dimensional section characteristics for use with strip theory.

The source distribution technique was developed by Frank (1967). The Frank approach has been very successful because of the wide variety of unusual forms that can be treated, e.g. bulbous bows, submerged bodies, and catamarans. Thus, certain bulbous bow shapes that are difficult to accurately represent with mapping techniques offer no special difficulties for the close-fit source distribution approach. The source distribution technique has been used in the most advanced ship motion work currently available. The work of Frank and Salvesen (1970) utilizes this technique for pitch and heave motion prediction. The most recent effort in the field by Salvesen, Tuck, and Faltinsen (1970) employs the source distribution technique to determine the hydrodynamic characteristics of a ship in all six degrees of freedom.

The original work by Frank is restricted to the deep-water case. However, problems such as operation of supertankers within near-shore waterways and naval vessels close to shore have created interest in the behavior of ships in finite depth waters. It is desirable, therefore, to extend the infinite depth fluid case to include the effects of water of finite depth. The first and most difficult requirement for this extension is to obtain a numerical method for predicting the velocity potential for a pulsating source of arbitrary strength in a fluid with a free surface and finite depth. With a suitable evaluation of this potential, the next step is to adapt it for use with a source distribution program such as that by Frank (1967). This will allow two-dimensional added-mass and damping characteristics to be predicted for a variety of shapes. Such data can then be used with strip theory to determine motions of various marine vehicles in a finite water depth environment.

The objective of this work is the development of a numerical technique to accomplish the first of the above steps. Specifically, the following efforts are presented:

1. Derivation of the velocity potential for a single pulsating source in a fluid with a free surface and finite depth.
2. A numerical technique for evaluation of the resultant potential.
3. Exploration of the following parameters:
 - a. Water depth h
 - b. Source submergence b
 - c. Pulsating frequency σ

In addition, it will be demonstrated that as the water depth increases, the solution tends toward that obtained for infinitely deep fluids.

The required finite depth velocity potential has been given by several investigators: John (1950), Wehausen and Laitone (1960), Thorne (1953) and Porter (1960). Both Wehausen and Laitone (1960) and also Porter (1960) provide detailed explanations of the procedure used to formulate the velocity potential for both the infinite and finite depth two-dimensional problems. Thorne (1953) also provides a good description of the procedures used to formulate the potential but gives considerably less detail.

Numerical evaluations of the finite depth potential for the purpose of finding added mass and damping have been attempted by several investigators with mixed success. Yu and Ursell (1961) used infinite series expansions of a type suggested by Thorne (1953) to allow comparison of experimental and theoretical wave amplitudes and obtained generally good agreement. McCreight (1970) experienced some difficulty with his numerical evaluation as depth increased, but he obtained good results for shallow water values of his depth

parameters. Porter (1960) experienced difficulty in the numerical evaluation of his finite depth potential and had to abandon the effort before the problems could be remedied. Kim (1969) appeared to have some difficulty in comparing his results with those of Yu and Ursell (1961), and his effort may contain some errors. Kim states that he employed the same expansions of the velocity potential as used by Yu and Ursell and one would expect their results to be in close agreement.

The technique used in this report to evaluate the velocity potential follows an approach due primarily to John (1950) and Wehausen and Laitone (1960), although the derivation of the potential in Appendix A follows an approach suggested by Thorne (1953). The form of the potential ultimately employed for numerical evaluation is slightly different than that suggested by Wehausen and Laitone (1960). The differences occur as a result of misprints in the text of the original reference. It is believed that the form of the finite depth potential is correct as given in later sections of this paper.

Subsequent sections and appendixes provide a formulation of the problem, a solution technique, a presentation of the effects resulting from prescribed variations of the problem parameters and a description and listing of a computer program. The results of the effort indicate that the representation and numerical evaluation technique obtained herein will allow a practical numerical calculation of the finite depth velocity potential that can be adapted for use with ship motion computer programs.

FORMULATION OF THE PROBLEM

The objective is to determine the velocity potential and then the free-surface elevation for the two-dimensional problem of a pulsating source of arbitrary strength fixed in a fluid of constant finite depth. The problem will be formulated in terms of potential-flow theory with a linearized free-surface condition. This approach allows the following assumptions:

1. The fluid is an ideal fluid, i.e., incompressible and inviscid.
2. Surface tension effects are negligible.
3. The motion amplitudes and the fluid velocities are small enough so that all but the linear terms in the free-surface and other boundary conditions may be neglected.

A complete discussion of linearized free-surface theory is provided by Stoker (1957).

A two-dimensional coordinate system with the y-axis pointing upward and the x-axis in the undisturbed free surface, as shown in Figure 1, is used as a reference for the problem formulation and numerical calculations.

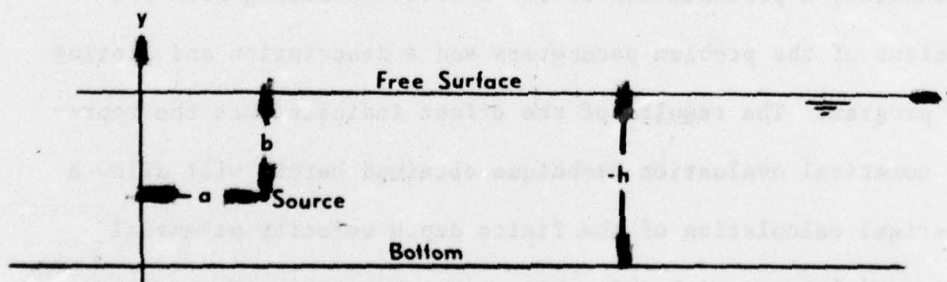


Figure 1 - Reference Coordinate System and Problem Geometry

An approach for solving this problem can now be formulated in terms of a velocity potential $\phi(x,y;t)$ which must satisfy the following linear boundary value problem:

1. The Laplace equation:

$$\phi_{xx} + \phi_{yy} = 0$$

except at (a, b).

2. The free-surface condition:

$$\phi_{tt} + g \phi_y = 0$$

on the undisturbed free surface, $y = 0$, where g denotes the acceleration of gravity.

3. The bottom condition:

$$\phi_y = 0 \text{ at } y = -h$$

4. The radiation condition, i.e., the waves are progressive and outgoing at large distances from the source. As derived in Appendix A, the velocity potential that satisfies the above conditions, is:

$$\begin{aligned} \phi(x,y;t) = & \frac{Q}{2\pi} \left[\log \frac{r_1}{h} + \log \frac{r_2}{h} - 2 \int_0^{\infty} \left\{ \frac{k+v}{k} \frac{e^{-kh} \cosh k(h+b) \cosh k(h+y) \cos k(x-a)}{k \sinh kh - v \cosh kh} \right. \right. \\ & \left. \left. + \frac{e^{-kh}}{h} \right\} dk \right] \cos \sigma t \\ & - Q \frac{v+m_0}{m_0} \frac{e^{-m_0 h} \sinh m_0 h \cosh m_0(h+b) \cosh m_0(y+h) \cos m_0(x-a)}{v h + \sinh^2 m_0 h} \sin \sigma t \end{aligned} \quad [1]$$

where Q is the source strength, a is the x -location of the source, b is the y -location of the source, t is the time, σ is the pulsating frequency, and h is the depth of the fluid. The remaining terms in Equation [1] are given by the following expressions:

$$v = \sigma^2/g$$

$$r = \sqrt{(x-a)^2 + (y-b)^2}$$

$$r_2 = \sqrt{(x-a)^2 + (y + 2h + b)^2}$$

m_0 is the root of the equation: $m_0 \tanh m_0 h = v$

The derivation of the potential expression in Appendix A follows a method outlined by Thorne (1953) for the infinite depth case. The form of the potential in Equation [1] is given by Wehausen and Laitone (1960) with slight modification. The two forms are equivalent, however, as is shown in Appendix A. The modification to the Wehausen and Laitone (1960) form of the potential involves a change of sign in one of the terms within the principal value integral. The change is indicated by an asterisk above the modified sign in Equation [1].

The free-surface elevation due to a submerged pulsating source was selected as the parameter most suitable for observing the influence of fluid depth, source submergence, and frequency. This was done because the free-surface elevation is a more easily recognized physical parameter than the value of the potential itself. According to potential-flow theory, the free-surface elevation is:

$$\eta(x,0;t) = -\frac{1}{g} \phi_t(x,0,t)$$

Numerical determination of the free-surface elevation requires that the potential be expressed in a form having "good" numerical behavior, that is, converging to a solution in a reasonable manner for all expected values of the physical parameters.

SOLUTION OF THE PROBLEM

Appendix B provides a brief explanation of the process involved in expressing the potential in terms of a series expansion which can be used for numerical computations. The resulting form of the potential is:

$$\phi(x,y;t) = \frac{2Q}{m_0} \left[\frac{(m_0 + \nu)e^{-m_0 h} \cosh m_0 h}{2m_0 h + \sinh 2m_0 h} \right] \cosh m_0(y+h) \cosh m_0(b+h) \sin(m_0|x-a| - \sigma t) - Q \sum_{k=1}^{\infty} \frac{m_k^2 + \nu + \nu^2}{m_k(hm_k^2 + h\nu^2 - \nu)} \cos m_k(y+h) \cos m_k(b+h) e^{-m_k|x-a|} \cos \sigma t \quad [2]$$

where m_k are the positive, real roots of the equation

$$m_k \tan m_k = -\nu$$

and m_0 is the positive, real root of the equation

$$m_0 \tanh m_0 = \nu$$

The free-surface elevation thus becomes:

$$\eta(x,0;t) = \frac{2Q\sigma}{m_0 g} \left[\frac{(m_0 + \nu)e^{-m_0 h} \cosh^2 m_0 h}{2m_0 h + \sinh 2m_0 h} \right] \cosh m_0(b+h) \cos(m_0|x-a| - \sigma t) - \frac{Q\sigma}{g} \sum_{k=1}^{\infty} \frac{m_k^2 + \nu^2}{m_k(hm_k^2 + h\nu^2 - \nu)} \cos m_k h \cos m_k(b+h) e^{-m_k|x-a|} \sin \sigma t \quad [3]$$

A computer program has been developed for numerical evaluation of Equation [3]. The details of the program are given in Appendix C.

PRESENTATION AND DISCUSSION OF RESULTS

The results of a study that systematically varied the value of the principal parameters, the water depth, the depth of the source below the free surface, and the frequency of oscillation are presented at the end of this section in Figures 2 - 5. The computations for a given wave form were performed for constant values of all the physical parameters, with the exception of the x-distance of the field point from the source. The x-distance was varied so that the wave form in the figures represents a "slice" of the wave at an instant in time. The source strength was unity for all computations.

Figure 2 provides a comparison of the wave form generated by using the finite depth program and that generated by using a previously developed infinite depth program. The conditions for the finite depth runs were:

h (water depth)	= 10 ft
b (source submergence)	= -3.0 ft
σ (frequency)	= 3.5 rad/sec

For the infinite depth runs, the source was located at -3.0 ft and the frequency was 3.5 rad/sec. The values of the time parameter selected for both programs were $t = 2.0196, 4.0392$ and 5.3851 sec. These values, in combination with the selected frequency, result in the σt term in Equation [3] assuming values of $\pi/4, \pi/2,$ and 0 respectively. Both phase and amplitude of the resultant wave forms may be compared by calculating the wave forms at several different values of time.

Figure 2 demonstrates that the infinite and finite depth results are in close agreement for selected conditions. There is a small difference in the wavelength (λ), with the finite depth wavelength equal to 16.4996 and the infinite depth wavelength equal to 16.5158. Otherwise, agreement between the wave forms generated by the two programs is quite close. Shown in Figure 2b as a dashed line is a 5-ft depth case with other conditions the same as for the 10-ft case. The results exhibit the expected characteristics: first, the wavelength is reduced ($\lambda = 15.8938$ versus $\lambda = 16.4996$) and second, the amplitude of the wave is increased.

Figure 3 illustrates the results of keeping water depth, frequency, and time constant while varying the depth of the source. For all of the runs in Figure 3, water depth was 6.0 ft, frequency was 3.5 rad/sec and time was 2.0196 sec whereas source submergence varied between -5.0 and -1.0 ft. The wavelength remains the same at all values of the source submergence because wavelength is a function of m_0 ($\lambda = 2\pi/m_0$), and m_0 is independent of the source submergence. The amplitude of the wave is dependent on the source submergence, however, as is the "range" of the significant influence of the logarithmic terms. The asterisk in Figure 3a indicates that the value of the term that contains both the principal value integral and the logarithmic terms is less than 0.0001 at an x-distance of 21.0 from the source for the -5.0 source submergence case. The asterisk in Figure 3e indicates that the corresponding point for the -1.0 source submergence case occurs at a somewhat smaller value of the x-distance ($x = 20.0$). In addition, the importance of the term as a percent of the total wave height is more significant for the $b = -5.0$ case than it is for the $b = -1.0$ case, thus the statement that the significant influence of the logarithmic terms is decreased as source submergence is reduced.

Figure 4 indicates the effect of varying the water depth while holding source submergence, frequency, and time constant. Water depth was varied between 5.0 and 3.0 ft while source submergence, frequency, and time were held constant and equal to -2.0 ft, 3.5 rad/sec, and 2.0196 sec, respectively.

The water depth affects both wave amplitude and wavelength. The wavelength becomes significantly shorter as depth decreases. In Figure 4a ($h = 5.0$) the wavelength is 15.8938 whereas in Figure 4c ($h = 3.0$) the wavelength is 14.3058. The wave amplitude increases as water depth decreases. Also, as water depth tends toward small values, the rate of increase in wave height becomes large.

Figure 5 shows the wave form that results from a lower frequency of oscillation. Part a of Figure 5 corresponds to part a of Figure 4 in all parameters except frequency. The wave form in Figure 5a is for a frequency of 2.5 whereas the wave form in Figure 4a is for a frequency of 3.5. The same correspondence exists between Figures 4b and 5b.

The lower frequency results in longer wavelengths and a slightly smaller amplitude compared with the higher frequency case. As in previous examples, the results shown in Figure 5 indicate that as water depth decreases, wavelength decreases and wave height increases. For the same change in parameters, however, the effects of depth on wavelength are slightly more noticeable for the lower frequency than for the higher frequency results. For example, the ratio of the wavelengths in Figures 4a and 4b was 1.04 whereas the corresponding ratio for Figures 5a and 5b was 1.08. A comparison of the amplitudes in Figures 4a and 5a shows that the wave amplitude for the lower frequency was less than that for the higher frequency (0.0472 versus 0.0460).

BEST AVAILABLE COPY

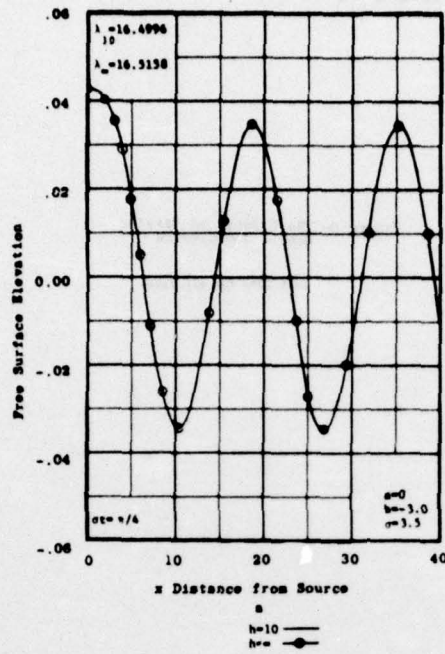
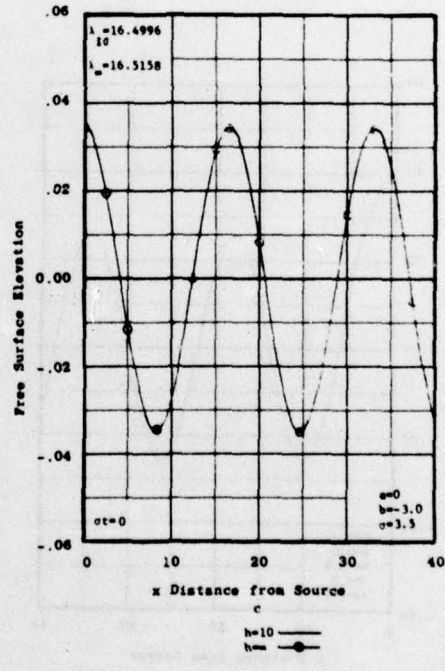
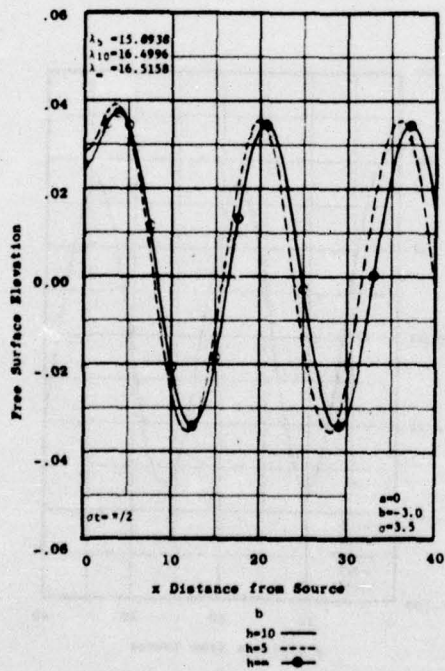


Figure 2- Comparison of Wave Form from the Finite and Infinite Depth Potentials



BEST AVAILABLE COPY

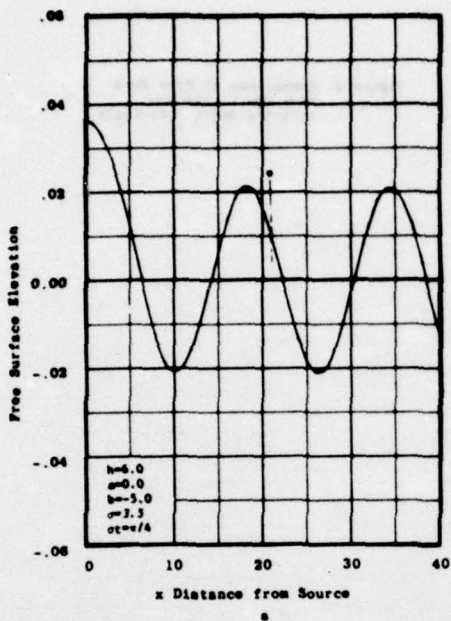
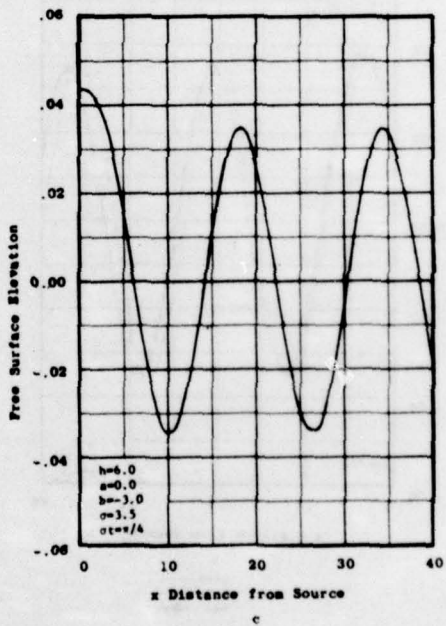
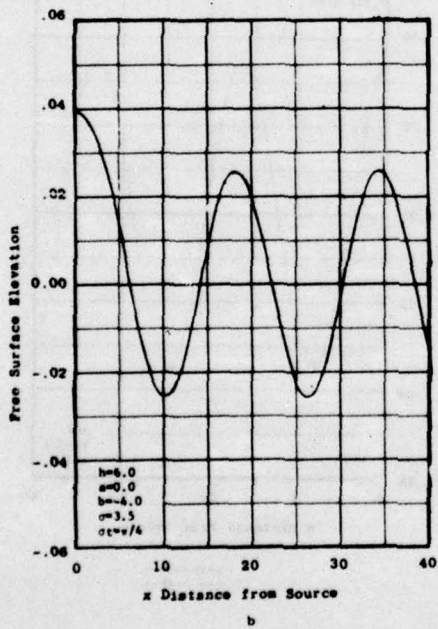


Figure 3- The Effects of Varying Source Submergence

$\lambda=16.2040$ for all cases



BEST AVAILABLE COPY

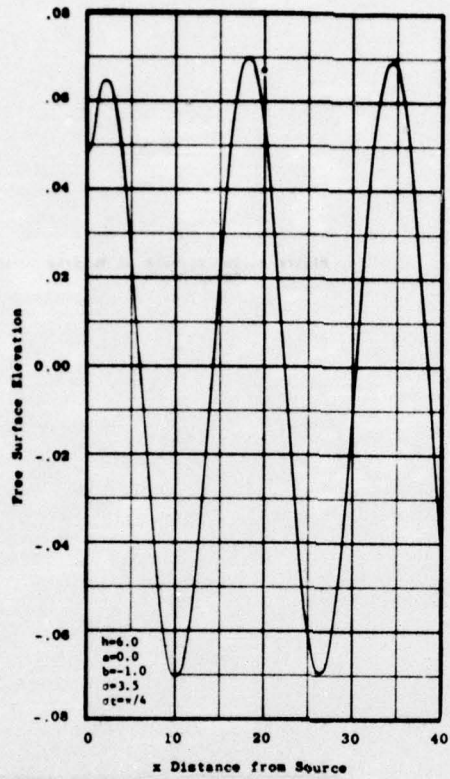
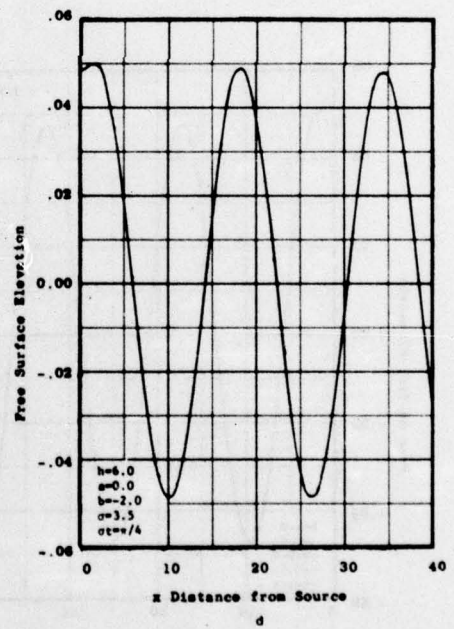


Figure 3- Continued



BEST AVAILABLE COPY

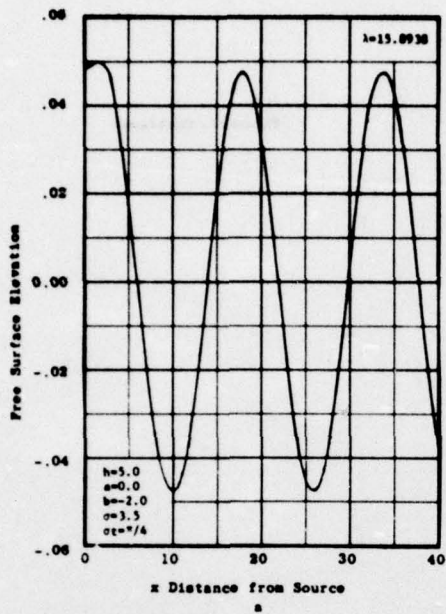
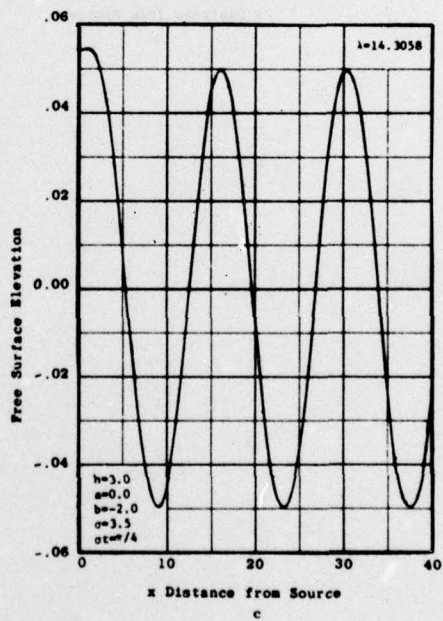
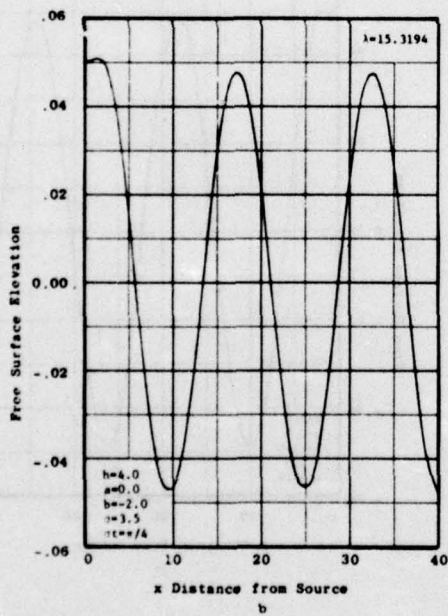


Figure 4- The Effects of Varying Water Depth



BEST AVAILABLE COPY

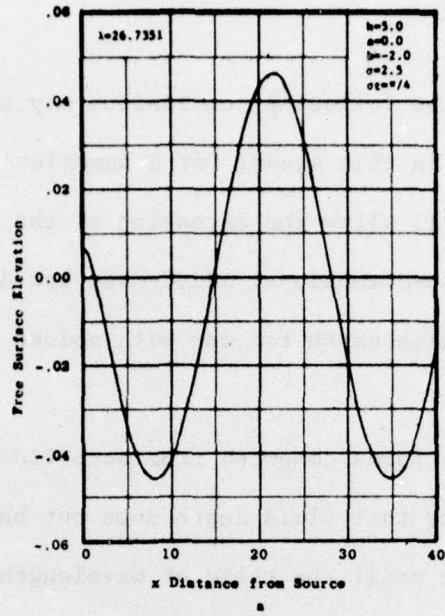
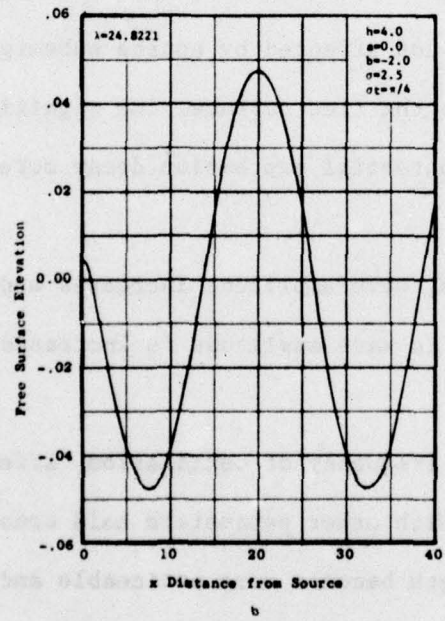


Figure 5- Lower Frequency Wave Form



CONCLUSIONS

As a result of this study, the following conclusions may be drawn:

1. The techniques employed in this study, for a numerical evaluation of the finite depth potential, will allow the extension of the source distribution method to provide two-dimensional added-mass and damping characteristics in a fluid of finite depth for use with modern ship motion strip theories.

2. Comparisons between wave forms computed from both finite and infinite depth potentials indicate that fluid depth does not begin to significantly alter the wave form until the ratio of wavelength to water depth is 1.7 or greater.

3. The deeper the submergence of the source, the lower the amplitude of the wave form. Wavelength is not affected by source submergence. Also, as the source is placed closer to the free surface, the significant effects of the logarithmic terms in the potential expression decay more rapidly with distance from the source.

4. As fluid depth decreases, wave amplitude increases and wavelength decreases. The rate of increase in wave amplitude is increased as fluid depth decreases.

5. Pulsating frequency, or frequency of oscillation, affects both wavelength and wave amplitude. With other parameters held constant, the effect of fluid depth on wavelength becomes more noticeable and wave amplitude is reduced as frequency is decreased.

ACKNOWLEDGMENTS

The author is grateful for much assistance and understanding afforded him by several individuals. Dr. Choung Mouk Lee, of the Ship Dynamics Division, spent many hours providing the author with valuable insights into free-surface problems and hydrodynamics in general. Dr. Nils Salvesen, of the Naval Hydrodynamics Division and of the George Washington University, provided excellent direction and identified several important problem areas in his capacity as thesis advisor. Mr. Vincent Monacella, also of the Ship Dynamics Division, provided guidance and much source information that proved invaluable in understanding the special topic of finite depth fluid mechanics and special numerical evaluation techniques. Sincere appreciation is extended to all of these kind and generous gentlemen.

BIBLIOGRAPHY AND REFERENCES

- Churchill, R.V., "Complex Variables and Applications," McGraw-Hill Book Company, New York, New York 1960.
- Frank, W., "Oscillation of Cylinders in or Below the Free Surface of Deep Fluids," NSRDC Report 2375, October 1967.
- Frank, W., and Salvesen, N., "The Frank Close-Fit Ship-Motion Computer Program," NSRDC Report 3289, June 1970.
- Gerritsma, I., "Distribution of Hydrodynamic Forces along the Length of a Ship Model in Waves," Technological University, Delft, Netherlands, Shipbuilding Laboratory Publication 144, 1966.
- Grim, O., "Berechnung der durch Schwingungen eines Schiffskoerpers Erzeugten Hydrodynamischen Kraefte," Fahrbuch der Schiffsbautecnischen Gesellschaft, Volume 47, 1953.
- Grim, O., "A Method for a More Precise Computation of Heaving and Pitching Motions both in Smooth Water and in Waves," Proceedings, Third Symposium on Naval Hydrodynamics, Scheverungen, Netherlands, 1960.
- Hildebrand, F.B., "Introduction to Numerical Analysis," McGraw-Hill Book Company, Inc., New York 1956.
- Hodgmen, C.D., (editor) "C. R. C. Standard Mathematical Tables," Chemical Rubber Publishing Company, Cleveland, Ohio, 1959.
- John, F., "On the Motion of Floating Bodies," Communications in Pure and Applied Mathematics, Volume 3, 1950.
- Kim, C.H., "Hydrodynamic Forces and Moments for Heaving, Swaying and Rolling Cylinders on Water of Finite Depth," Chalmers University of Technology, Division of Ship Hydromechanics Report Number 43, April 1968.
- Kim, C.H., "The Influence of Water Depth on the Heaving and Pitching Motion of a Ship Moving in Longitudinal Regular Head Waves," Chalmers University of Technology, Division of Ship Hydromechanics Report Number 44, June 1968.
- Kim, C.H., "The Influence of Water Depth on the Midship Bending Moments of Ship Moving in Longitudinal Regular Head Waves," European Shipbuilding, Number 1, 1969.
- Kim, C.H., "Hydrodynamic Forces and Moments for Heaving, Swaying and Rolling Cylinders on Water of Finite Depth," Journal of Ship Research, Volume 13, Number 2, June 1969.

- Korvin-Kroukovsky, B.V. and Jacobs, W.R., "Pitching and Heaving Motions of a Ship in Regular Waves," Transactions, Society of Naval Architects and Marine Engineers, Volume 65, 1957.
- Monacella, V.J., "On Ignoring the Singularity of the Numerical Evaluation of Cauchy Principal Value Integrals," NSRDC Report 2356, February 1967.
- Ogilvie, T.F., "First and Second Order Forces on a Cylinder Submerged Under a Free Surface," Journal of Fluid Mechanics, Volume 16, Part 3, 1963.
- Porter, W.R., "Pressure Distributions, Added-Mass and Damping Coefficients for Cylinders Oscillating in a Free Surface," University of California (Berkeley) Institute Engineering Research, Series 82, Issue 16, 1960.
- Salvesen, N., "On Second-Order Wave Theory for Submerged Two-Dimensional Bodies, University of Michigan Report IP-736, April 1966.
- Salvesen, N., Tuck, O.E., and Faltinsen, O., "Ship Motions and Sea Loads," Transactions, Society of Naval Architects and Marine Engineers, Volume 78, 1970.
- Smith, W.E., "Computation of Pitch and Heave Motions for Arbitrary Ship Forms," Technological University, Delft, Netherlands, Shipbuilding Laboratory Publication 148, 1966.
- Stoker, J.J., "Surface Waves in Water of Variable Depth," Quarterly of Applied Mathematics, Volume 5, No. 1, April 1947.
- Stoker, J.J., "Water Waves," Interscience Publishers, Inc., New York, New York, 1957.
- Thorne, R.C., "Multipole Expansions in the Theory of Surface Waves," Proceedings of the Cambridge Philosophical Society, Volume 49, Number 707, 1953.
- Ursell, F., "On the Heaving Motion of a Cylinder on the Surface of a Fluid," Quarterly Journal of Mechanics and Applied Mathematics, Volume 2, 1949.
- Ursell, F., "Water Waves Generated by Oscillating Bodies," Quarterly Journal of Mechanics and Applied Mathematics, Volume 7, 1954.
- Ursell, F., Dean R.G., and Yu, Y.S., "Forced Small-Amplitude Water Waves: A Comparison of Theory and Experiment," Journal of Fluid Mechanics, Volume 7, 1954.
- Wehausen, J.V., and Laitone, E.V., "Surface Waves," Encyclopedia of Physics, Fluid Dynamics III, Volume 9, edited by S. Fluegge, Springer-Verlag, Berlin, Germany, 1960.

Wigley, C.W., "The Collected Papers of Sir Thomas Havelock on Hydrodynamics,"
Office of Naval Research Department of the Navy, ONR/ACR-103, U.S. Government
Printing Office, Washington, D.C., 1965.

Yu, Y.S. and Ursell, F., "Surface Waves Generated by an Oscillating Circular
Cylinder on Water of Finite Depth: Theory and Experiment," Journal of
Fluid Mechanics, Volume 11, 1961.

APPENDIX A

DERIVATION OF THE VELOCITY POTENTIAL FOR WATER OF FINITE DEPTH

The derivation of the velocity potential for a source pulsating in a fluid with free surface and finite depth is presented in this appendix. The derivation follows a method suggested by Thorne (1953) for the infinite depth case. However, the computer program used to evaluate the potential is based on a form due to John (1950) and elaborated on by Wehausen and Laitone (1960). The two forms are equivalent, however, as will be shown at the end of this appendix.

COORDINATE SYSTEM AND IDENTIFICATION OF PHYSICAL PARAMETERS

Figure A.1 shows the coordinate system used for the derivation and illustrates the basic geometric parameters. The y-axis is positive downward and the x-axis is in the undisturbed free surface of the fluid.

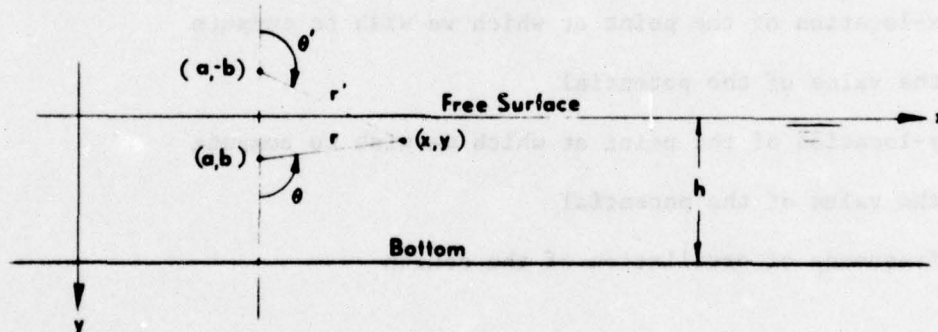


Figure A.1 - Coordinate System and Problem Geometry for Derivation
of the Potential Expression

The coordinate system is the same as employed by Thorne (1953) but different than that employed by Wehausen and Laitone (1960). The latter employ a system that has the y-axis positive in the upward direction, as shown in Figure 1. The computer program also employs the coordinate system shown in Figure 1 and not the one given in this appendix.

The physical parameters are defined as follows:

h = depth of fluid as measured from the mean free surface to the bottom; the bottom is assumed to be uniform

a = x-location of the source

b = y-location of the source

θ = $\tan^{-1} (x-a)/(y-b)$

θ' = $\tan^{-1} (x-a)/(y+b)$

r = $\sqrt{(x-a)^2 + (y-b)^2}$

r' = $\sqrt{(x-a)^2 + (y+b)^2}$

x = x-location of the point at which we wish to compute the value of the potential

y = y-location of the point at which we wish to compute the value of the potential

σ = frequency of oscillation of the source

STATEMENT OF PROBLEM

Since this analysis is for the two-dimensional case, the singularity will be logarithmic in form. The statement of the problem has been presented in the main text, but it is repeated here for continuity of presentation.

and because of the possible confusing over the different coordinate systems.

We seek a function of the form

$$\phi(x,y;t) = \phi_1(x,y)\cos \sigma t + \phi_2(x,y)\sin \sigma t \quad [A-1]$$

defined for $y \geq 0$, except at (a,b) and satisfying the conditions

1. $\nabla^2 \phi_i = 0$, $i = 1,2$, except at (a,b)
2. $v\phi_i + \frac{\partial \phi_i}{\partial y} = 0$, $i = 1,2$, $v = \sigma^2/g$
3. $\frac{\partial \phi_i}{\partial y} = 0$, $i = 1,2$, at $y = h$
4. The radiation condition, i.e., the waves are outgoing as x tends to infinity
5. $\phi_1(x,y) = \log r/r' + \phi_0(x,y)$

DERIVATION OF POTENTIAL

Thorne (1953) suggested the following form for the $\phi_0(x,y)$ potential:

$$\phi_0(x,y) = \int_0^{\infty} [A(k)\sinh ky + B(k)\cosh k(h-y)] \cos k(x-a) dk \quad [A-2]$$

This is a harmonic function that satisfies condition 1 since

$$\begin{aligned} \phi_{0xx} &= \int_0^{\infty} -k^2 [A(k)\sinh ky + B(k)\cosh k(h-y)] \cos k(x-a) dk \\ \phi_{0yy} &= \int_0^{\infty} k^2 [A(k)\sinh ky + B(k)\cosh k(h-y)] \cos k(x-a) dk \end{aligned}$$

and hence $\phi_{0xx} + \phi_{0yy} = 0$. The $\phi_2(x,y)$ potential will be determined later

to satisfy the radiation condition (Item 4). The function $A(k)$ and $B(k)$

must be chosen such that the integral in [A-2] converges in the region

$$-\infty < x < \infty, 0 \leq y \leq h$$

To accomplish this task, the expression for $\phi_1(x,y)$ is put into the

free-surface condition (Item 2) to give:

$$\frac{\partial}{\partial y} \log \frac{r}{r'} + v \log \frac{r}{r'} + \frac{\partial}{\partial y} \int_0^{\infty} [A(k) \sinh ky + B(k) \cosh k(h-y)] \cos k(x-a) dk + v \int_0^{\infty} [A(k) \sinh ky + B(k) \cosh k(h-y)] \cos k(x-a) dk = 0 \quad [A-3]$$

At $y = 0$, the following is true from consideration of the geometry of the problem:

$$\frac{\partial}{\partial y} \log \frac{r}{r'} = \frac{-2b}{(x-a)^2 + b^2} \quad [A-4]$$

The derivative in [A-3] may be expressed as follows

$$\begin{aligned} & \frac{\partial}{\partial y} \int_0^{\infty} [A(k) \sinh ky + B(k) \cosh k(h-y)] \cos k(x-a) dk \\ & = \int_0^{\infty} [kA(k) \cosh ky - kB(k) \sinh k(h-y)] \cos k(x-a) dk \end{aligned} \quad [A-5]$$

Substituting the [A-4] and [A-5] relations into [A-3] for $y = 0$ gives

$$\int_0^{\infty} \{kA(k) - B(k) [k \sinh kh - v \cosh kh]\} \cos k(x-a) dk = \frac{2b}{(x-a)^2 + b^2} \quad [A-6]$$

The "well-known" identity*

$$\int_0^{\infty} e^{-\beta x} \cos mx dx = \frac{\beta}{m^2 + \beta^2} \quad \text{for } \beta > 0$$

can be written in terms of the problem variables as

$$2 \int_0^{\infty} e^{-kb} \cos k(x-a) dk = \frac{2b}{(x-a)^2 + b^2}$$

Using this identity with Equation [A-6] and equating the integrands of the resulting integral expressions gives the following equation in $A(k)$ and $B(k)$:

* See Hodgmen (1959), page 314, number 430.

$$B(k) = \frac{-kA(k) + 2e^{-kb}}{-k \sinh kh + v \cosh kh} \quad [A-7]$$

Consider now the bottom condition (Item 3). The final form of the function must satisfy this condition for $y = h$. At $y = h$, the problem geometry gives:

$$\begin{aligned} \frac{\partial}{\partial y} \log \frac{r}{r'} &= \frac{h-b}{(x-a)^2 + (h-b)^2} - \frac{h+b}{(x-a)^2 + (h+b)^2} \\ &= \int_0^{\infty} \left[e^{-k(h-b)} - e^{-k(h+b)} \right] \cos k(x-a) dk \end{aligned} \quad [A-8]$$

Setting $y = h$ in Equation [A-5] and equating the right-hand side of this expression to the integral in [A-8] yields the integral equation

$$\int_0^{\infty} kA(k) \cosh kh \cos k(x-a) dk = -2 \int_0^{\infty} e^{-kh} \cosh kb \cos k(x-a) dk \quad [A-9]$$

It can now be observed that in order to satisfy the bottom condition the following must be true:

$$A(k) = \frac{-2e^{-kh}}{k \cosh kh} \sinh kb \quad [A-10]$$

The combination of Equations [A-7] and [A-10] provides an explicit expression for $B(k)$:

$$B(k) = \frac{2(e^{-kh} \sinh kb + e^{-kb} \cosh kh)}{\cosh kh (k \sinh kh + v \cosh kh)} \quad [A-11]$$

Introducing the expressions for $A(k)$, [A-10], and $B(k)$, [A-11], into Equation [A-2] gives the desired expression for the potential:

$$\phi_0(x, y) = 2 \int_0^{\infty} \left\{ \frac{\cosh k(h-b) \cosh k(h-y)}{\cosh kh (v \cosh kh - k \sinh kh)} - \frac{e^{-kh} \sinh kb \sinh ky}{k \cosh kh} \right\} \cos k(x-a) dk \quad [A-12]$$

The next step is to determine $\phi_2(x,y)$, which is the second term in the potential expression in [A-1]; $\phi_2(x,y)$ must be selected such that $\phi(x,y;t)$ represents an outgoing wave as x tends to infinity (the radiation condition). To accomplish this step, the form of the ϕ_1 potential for large values of x must be found. This requires evaluation of the integral in [A-12] around a contour formed by the quadrant $R(k) > 0, I(k) > 0$ but excluding any singularities that occur along the $R(k)$ axis. Figure A.2 shows such a contour.

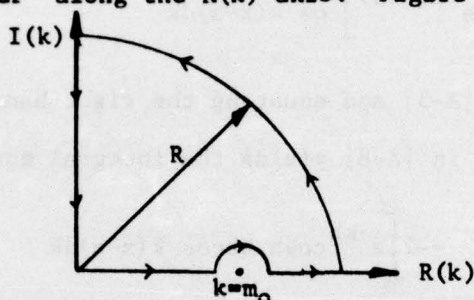


Figure A.2 - Contour of Integration

It is convenient to rewrite the integral express for $\phi_0(x,y)$ differently than that shown in [A-12] to give:

$$2 \int_0^{\infty} \left[\frac{k \cosh k(h-b) \cosh k(h-y) - e^{-kh} \sinh k b \sinh ky (\nu \cosh kh - k \sinh kh)}{k \cosh kh (\nu \cosh kh - k \sinh kh)} \right] \cdot \cos k(x-a) dk$$

$$= 2 \int_0^{\infty} \frac{p(k)}{q(k)} \cos k(x-a) dk \quad [A-13]$$

We are concerned with the case where k is greater than zero. The only singularity in the integral expression, [A-13], therefore, occurs at the value of $k = m_0$, where m_0 is the positive, real root of the equation:

$$\nu \cosh kh - k \sinh kh = 0 \quad [A-14]$$

The integral expression in [A-13] may now be written as the sum of the integrals along the parts of the contour of integration plus the value of the residue term at $k = m_0$:

$$\begin{aligned}
 \frac{1}{2} \operatorname{Real} \left\{ \int_0^{\infty} \frac{p(k)}{q(k)} e^{-ikx} dk \right\} &= \operatorname{Real} \left\{ \int_0^{\infty} \frac{p(\beta)}{q(\beta)} e^{i\beta x} d\beta \right. \\
 &\quad \left. - i\pi [\operatorname{Residue}] e^{im_0 x} \right. \\
 &\quad \left. - i \int_0^{\infty} \frac{p(in)}{q(in)} e^{-nx} dn \right. \\
 &\quad \left. + \int_0^{\pi/2} \frac{p(\operatorname{Re}^{i\theta})}{q(\operatorname{Re}^{i\theta})} e^{i\operatorname{Re}^{i\theta} x} d(\operatorname{Re}^{i\theta}) \right\}
 \end{aligned}
 \tag{A-15}$$

where along the axes

$$\begin{aligned}
 k = \beta + in, \quad dk = d\beta \quad \text{for} \quad \longrightarrow \bullet \longrightarrow \\
 dk = idn \quad \text{for} \quad \downarrow
 \end{aligned}$$

and along the arc

$$k = \operatorname{Re}^{i\theta}, \quad dk = i\operatorname{Re}^{i\theta} d\theta$$

$$R > 0, \quad 0 \leq \theta \leq \pi/2$$

The individual expressions in [A-15] are now examined.

The integral along the arc

$$\int_0^{\pi/2} \frac{p(\operatorname{Re}^{i\theta})}{q(\operatorname{Re}^{i\theta})} e^{ix\operatorname{Re}^{i\theta}} i\operatorname{Re}^{i\theta} d\theta$$

tends toward zero as $R \rightarrow \infty$.

The integral along the imaginary axis

$$-i \int_0^{\infty} \frac{p(i\eta)}{q(i\eta)} e^{-\eta x} d\eta$$

tends toward zero as $x \rightarrow \infty$.

The integral along the real axis is the principal value integral we seek to evaluate. The integral on the left-hand side of [A-15] is an integral about a closed analytic region and is zero by the Cauchy integral theorem. The value of the residue term is determined in the following manner:

Define

$$f(k) = \frac{p(k)}{q(k)} \quad \text{and } b_1 = \text{the residue at } k = m_0$$

According to Churchill (1960), the residue of $f(k)$ due to a singularity at $k = m_0$ exists if

- a. $p(m_0) \neq 0$
- b. $q(m_0) \neq 0$
- c. $q'(m_0) \neq 0$

Since m_0 is defined as the root of the $q(k)$ function and $q(m_0) = 0$, condition b is satisfied. Likewise condition a is satisfied since $p(m_0) \neq 0$ if $k > 0$, and such a restriction on k has already been specified. The expression for $q'(k)$ must be examined to determine whether condition c is met by the $f(k)$ function. Now, $q'(k)$ may be expressed as:

$$q'(k) = v \cosh^2 kh + 2kvhsinh kh \cosh kh \\ - k \sinh 2kh - k^2 h \cosh 2kh$$

Also, at $k = m_0$,

$$v = m_0 \frac{\sinh m_0 h}{\cosh m_0 h} \quad \text{and} \quad q'(m_0) = \frac{-m_0}{2} \sinh m_0 h + m_0^2 h$$

In order to satisfy condition c the expression

$$\sinh 2m_0 h + 2m_0 h \neq 0 \quad [\text{A-16}]$$

must be true. The only root of Equation [A-16] occurs at $2m_0 h = 0$ or at $m_0 = 0$ since h is always greater than zero. The value of m_0 cannot be zero if h is greater than zero and therefore condition c is satisfied. The residue term in Equation [A-15] thus becomes

$$b_1 = \frac{-2 \cosh m_0 (h-b) \cosh m_0 (h-y)}{2m_0 h + \sinh 2m_0 h} \quad [\text{A-17}]$$

All of the integrals and terms in Equation [A-15] have now been evaluated.

Taking the real part of the resultant form of the integral yields an expression that is introduced into the potential function, Equation [A-12], to yield the following form for $\phi_0(x,y)$ for large x :

$$\phi_0(x,y) = \frac{4\pi \cosh m_0 (h-b) \cosh m_0 (h-y)}{2m_0 h + \sinh 2m_0 h} \sin m_0 x \quad [\text{A-18}]$$

As x becomes large, the logarithmic terms dissipate rapidly. This means that the sum of $\phi_0(x,y)$ and $\phi_2(x,y)$ must combine to ensure that the radiation condition (Item 4) is satisfied. A function that performs this task is:

$$\phi_2(x,y) = \frac{-4\pi \cosh m_0 (h-b) \cosh m_0 (h-y)}{2m_0 h + \sinh 2m_0 h} \cos m_0 x \quad [\text{A-19}]$$

All of the functions required to obtain the total velocity potential expression are now available.

Introducing $\phi_0(x,y)$, Equation [A-12], $\phi_2(x,y)$, Equation [A-19], and the logarithmic terms into Equation [A-1] provides an expression for

the velocity potential that satisfies all requirements and constraints:

$$\begin{aligned} \phi(x,y;t) = \frac{Q}{2\pi} \left[\log \frac{r}{r'} + 2 \int_0^{\infty} \left\{ \frac{\cosh k(h-b)\cosh k(h-y)}{\cosh kh(\cosh kh - k\sinh kh)} \right. \right. \\ \left. \left. - \frac{e^{-kh} \sinh kh \sinh ky}{k \cosh kh} \right\} \cos k(x-a) dk \right] \cos \sigma t \\ - \frac{2Q \cosh m_0(h-b) \cosh m_0(h-y)}{2m_0 h + \sinh 2m_0 h} \cos m_0(x-a) \sin \sigma t \end{aligned} \quad [A-20]$$

This is the same as the form derived by Thorne (1953).

ALTERNATE FORM FOR THE VELOCITY POTENTIAL

The most convenient form for the velocity potential is not the one expressed by Equation [A-20]. Because of planned adaptations of the numerical evaluation of the potential, a form given by Wehausen and Laitone (1960) is more desirable. The principal differences between the two alternate forms stem from the reference coordinate systems employed by the individual investigators. As mentioned previously, Thorne (1953) employs a coordinate system with the y-axis positive in the downward direction, as shown in Figure A.1. Wehausen and Laitone (1961), however, base their potential on a coordinate system with the y-axis positive in the up direction as shown in Figure 1. Other differences are due to slightly differing methods of representing geometric parameters. To convert from the potential form in Equation [A-20] to the equivalent expression as given by Wehausen and Laitone (1960) requires the following transformations and identities:

$$y = -y, \quad x = x$$

$$a = a, \quad b = -b$$

$$h = h$$

$$\int_0^{\infty} \frac{1 - \cos r\mu}{\mu} e^{-\beta\mu} d\mu = \log \frac{(r^2 + \beta^2)^{1/2}}{\beta}, \quad \beta > 0$$

$$\int_0^{\infty} \frac{e^{-\beta\mu} - e^{-h\mu}}{\mu} d\mu = \log \frac{h}{\beta}, \quad \beta > 0$$

[A-21]

$$\frac{e^{-m_0 h} \sinh m_0 h}{v h + \sinh^2 m_0 h} = \frac{2e^{-m_0 h} \cosh m_0 h}{2m_0 h + \sinh 2m_0 h} = \frac{m_0 - v}{h m_0^2 - h v^2 + v}$$

Substitution of [A-21] into [A-20] and algebraic manipulation results in the desired form of the velocity potential:

$$\phi(x, y; t) = \frac{Q}{2\pi} \left[\log \frac{r}{h} + \log \frac{r_2}{h} - 2 \int_0^{\infty} \left\{ \frac{k+v}{k} \frac{e^{-kh} \cosh k(h+b) \cosh k(y+h)}{k \sinh kh - v \cosh kh} \cos k(x-a) + \frac{e^{-kh}}{k} \right\} dk \right] \cos \sigma t$$

[A-22]

$$-Q \frac{v+m_0}{m_0} \frac{e^{-m_0 h} \sinh m_0 h \cosh m_0(h+b) \cosh m_0(y+h) \cos m_0(x-a)}{v h + \sinh^2 m_0 h} \sin \sigma t$$

$$\text{where } r = \sqrt{(x-a)^2 + (y-b)^2}$$

$$r_2 = \sqrt{(x-a)^2 + (y+2h+b)^2}, \text{ and } y \text{ is positive upward.}$$

The source is thus located at a distance $y=b$ beneath the free surface and the bottom is located at a $y=-h$ distance from the free surface.

APPENDIX B

SERIES EXPANSIONS USED TO NUMERICALLY EVALUATE THE VELOCITY POTENTIAL

A brief outline of the procedure used to derive a series expansion for the finite depth velocity potential is provided in this appendix. A more detailed explanation may be found in John (1950).

The integral expression for the potential is given by equation [A-22] but is repeated here for convenience:

$$\phi(x,y;t) = \frac{Q}{2\pi} \left[\log \frac{r_1}{h} + \log \frac{r_2}{h} - 2 \int_0^{\infty} \left\{ \frac{k+v}{k} \frac{e^{-kh} \cosh k(h+b) \cosh k(y+h) \cos k(x-a)}{k \sinh kh - v \cosh kh} - \frac{e^{-kh}}{k} \right\} dk \right] \cos \sigma t$$

[A-22]

$$- \frac{Q \frac{v+m_0}{m_0} e^{-m_0 h} \sinh m_0 h \cosh m_0(h+b) \cosh m_0(y+h) \cos m_0(x-a)}{vh + \sinh^2 m_0 h} \sin \sigma t$$

The first step is to express the coefficient of the $\sin \sigma t$ term in the potential expression, equation [A-22], in a different form through use of the following identity:

$$\frac{e^{-m_0 h} \sinh m_0 h}{vh + \sinh^2 m_0 h} = \frac{m_0 - v}{hm_0^2 - hv^2 + v}$$

Next, the identities provided by equations [A-21] are used to include the logarithmic terms under the integral in the coefficient of the $\cos \sigma t$ term in equation [A-22]. The integrand of the resulting integral is now expressed in the form of a partial fraction expansion and integrated term by term. The resultant expression for the potential is:

$$\begin{aligned} \phi(x,y;t) &= \frac{Q}{m_0} \frac{m_0^2 - v}{hm_0^2 - hv^2} \cosh m_0(y+h) \cosh m_0(b+h) \sin(m_0|x-a| - \sigma t) \\ &\quad - Q \sum_{k=1}^{\infty} \frac{1}{m_k} \frac{m_k^2 + v^2}{hm_k^2 + hv^2 - v} \cos m_k(y+h) \cos m_k(b+h) e^{-m_k|x-a|} \cos^* \sigma t \end{aligned} \quad [B-1]$$

where m_0 is the positive real root of the equation

$$m_0 \tanh m_0 h = v$$

and m_k are the positive, real roots of the equation

$$m_k \tan m_k h = -v$$

The asterisk under the $\cos \sigma t$ in equation [B-1] indicates that this term differs from the corresponding term in the expression given by Wehausen and Laitone.

An expression for the free-surface elevation may now be found by recalling that

$$\eta(x,0;t) = -\frac{1}{g} \phi_t \quad [B-2]$$

Introducing the time derivative of the potential expression in equation [B-2] results in the following equation for the free-surface elevation:

$$\begin{aligned} \eta(x,0;t) &= \frac{Q\sigma}{gm_0} \frac{m_0^2 - v^2}{hm_0^2 - hv^2 + v} \cosh m_0 h \cosh m_0(b+h) \cos(m_0|x-a| - \sigma t) \\ &\quad - \frac{Q\sigma}{g} \sum_{k=1}^{\infty} \frac{1}{m_k} \frac{m_k^2 + v^2}{hm_k^2 + hv^2 - v} \cos m_k h \cos m_k(b+h) e^{-m_k|x-a|} \sin \sigma t \end{aligned} \quad [B-3]$$

A slightly different form of this expression was adopted for use with the computer program. This form employs the identity

$$\frac{2e^{-m_0 h} \cosh m_0 h}{2m_0 h + \sinh 2m_0 h} = \frac{m_0 - \nu}{hm_0^2 - h\nu^2 + \nu}$$

to change the form of the first term in equation [B-3]. The final expression for the free-surface elevation, as programmed, is:

$$\begin{aligned} \eta(x, \sigma; t) = & \frac{2Q\sigma}{m_0 g} \frac{(m_0 + \nu)e^{-m_0 h} \cosh^2 m_0 h}{2m_0 h + \sinh 2m_0 h} \cosh m_0(b+h) \cos(m_0|x-a| - \sigma t) \\ & - \frac{Q\sigma}{g} \sum_{k=1}^{\infty} \frac{1}{m_k} \frac{m_k^2 + \nu^2}{hm_k^2 + h\nu^2 - \nu} \cos m_k h \cos m_k(b+h) e^{-m_k|x-a|} \sin \sigma t \end{aligned} \quad [B-4]$$

This representation is valid for $b > 0$, $h > 0$, and $r \neq 0$.

APPENDIX C

COMPUTER PROGRAM, LISTING, SAMPLE INPUT AND SAMPLE OUTPUT

The computer program has been assembled for use with a CDC 6700 computer and is written in the Fortran IV language. The program is easily adaptable to any modern high-speed computer with only minor changes in the Fortran IV program listing. No special input, output, or external storage devices are required. The program consists of one main program and two subroutines. The total program is entitled FINDEP; a listing is provided at the end of this appendix.

MAIN PROGRAM

The main program performs all input, output, and most of the numerical calculations involved in determining the free-surface elevation. The potential itself is not actually determined, but the program could be easily modified to provide such data.

The infinite sum term found in equation [B-4] is evaluated to N number of terms in the main program. A convergence criterion, stated below, determines the value of N for each value of x at which computations are performed. For computational purposes, the value of all parameters were considered constant except the x-distance of the field point from the source. The resultant wave form, therefore, represents a "slice" of the wave at an instant in time.

The convergence criterion of the infinite series is based on the difference between the average values of the summation term. Figure C.1

shows a typical plot of the term $\text{PHI2}(k)$ versus k for $x = a = 0$. The symbol $\text{PHI2}(k)$ represents the sum of the individual terms in the infinite series. As can be observed in the figure, convergence of the series to a representative value is quite slow. An estimate of the convergence value is made by determining the maximum and minimum values of $\text{PHI2}(k)$, taking the average of these numbers, and returning the value of the last average when the difference between previous averages is less than or equal to 0.0001. The value of N at which the criterion is met is the number of terms at which the series is truncated. If the convergence criterion is not met by the time $N = 189$, the average of the last minimum and last maximum value is returned. Thus, the value of N never exceeds 189.

For values of $(x-a)$ not equal to zero, the series convergence is greatly accelerated because of the rapid decay of the exponential term.

SUBROUTINE ROOT1

The ROOT1 subroutine computes the root, n , of the transcendental equation

$$n \tanh n = B$$

where $n = m_0 h$ and $B = v h$. The technique used to solve the equation employs the "Newton-Raphson" iteration technique with a convergence criterion that requires the incremental estimate for the root to be less than or equal to 0.0001. The "Newton-Raphson" technique works quite well and a suitably accurate root is generally attained within seven iterations. Figure C.2 presents a representative graphical solution to the equation for hypothetical problem parameters. It is clear from the figure that as B gets large, the value of B/n approaches 1.0, and that the root will always be positive and real. A detailed description of the "Newton-Raphson" technique is given in Hildebrand (1956).

SUBROUTINE ROOT2

The ROOT2 subroutine computes N number of roots of the transcendental equation

$$s \tan s = -B$$

where $s = m_k h$ and $B = v h$. As with subroutine ROOT1, the "Newton-Raphson" iteration technique is employed to determine the value of each of the required N number of roots.

Figure C.3 provides a representative plot of a graphical solution to the subject equation for typical values of the problem parameters. The positive, real roots of the equation are sought, and the roots must therefore lie in the second and fourth quadrants where the tangent function is negative. As s gets large, the value of the root approaches $k\pi$, where k is the summation index as shown in equation [B-4].

INPUT

The required input is identified below together with the data card requirements. Two data cards are required.

Data Card 1 (7F10.4)

The following floating point parameter values provide input via data card 1. They are listed in the order in which they must appear on the card.

- | | |
|-------------------------------|-----------------------------|
| 1. Q = source strength | 4. H = water depth |
| 2. G = gravitational constant | 5. A = x-location of source |
| 3. F = frequency | 6. B = y-location of source |
| | 7. T = time |

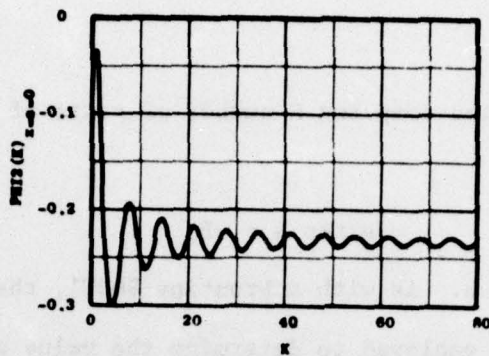


Figure C.1-Summation Term versus the Number of Terms in the Sum for the $x=0$ Case

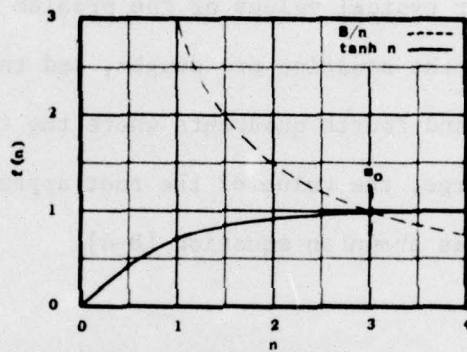


Figure C.2-Representative Graphical Solution for the Equation $n \tanh n = B$

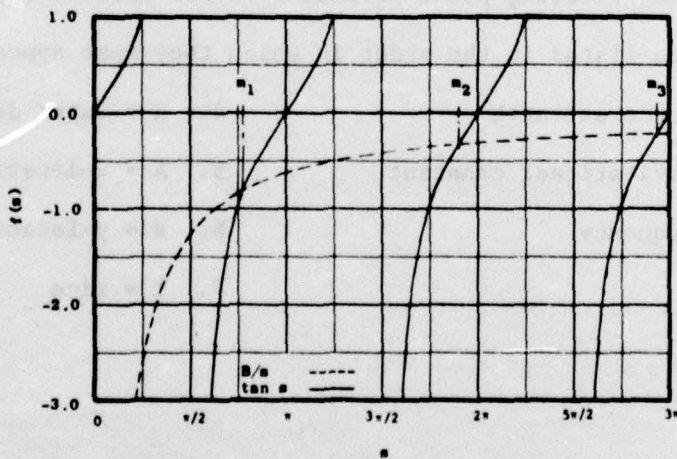


Figure C.3-Representative Graphical solution for the equation $s \tan s = -B$

Data Card 2 (F10.4, 16)

The parameters that provide input via data card 2 are as follows:

1. STEPX = incremental value of x
2. STEPY = incremental value of y
3. STEPZ = number of points at which the free-surface elevation will be calculated plus 1

The size of the increment step within the range of x is determined by STEPX. The value of STEPY must always be zero. The value of (STOPZ-1) determines the range of the calculation. Thus, the number of values of x at which the elevation will be calculated, M, is

$$(\text{STOPZ}-1) \cdot \text{STEPX} = M$$

For the present intended use of the program, inclusion of an iteration on y is not necessary. It was included, however, because of planned extensions to the program that include the calculation of the velocity potential at points other than on the free surface.

The program is constructed such that all calculations start at a value of x = 0.0.

SAMPLE INPUT AND OUTPUT

A sample set of parameter values and constants is identified below in terms of the variables in equation [B-4].

Data Card 1 Q = 1.0, g = 32.2, b = 3.5
 h = 6.0, a = 0.0, b = -4.0, t = 2.0196

Data Card 2 Incremental value of x = 1.0
 Incremental value of y = 0.0
 Range of x values + 1 = 42

The results of operating the program with the above input values are shown in the "OUTPUT" listing at the end of this appendix. Other than titles and identifications, the first information output is a listing of the input data. Certain interim calculation terms are printed next:

$$\begin{aligned} \text{SIGMA} &= \sigma^2/g \\ \text{GMU} &= m_0 \\ \text{ANGL1} &= \cosh m_0(b+h) \\ \text{SINF} &= \sin \sigma t \\ \text{COEF1A} &= \frac{m_0 + v}{m_0} e^{-m_0 h} \cosh m_0 h \\ \text{COEF1B} &= \frac{\cosh m_0(b+h)}{2m_0 h + \sinh 2m_0 h} \\ \text{COEF1} &= 2 * \text{COEF1A} * \text{COEF1B} \end{aligned}$$

and the calculated wavelength. The final output list includes the listing of the wave height as a function of x and y, the number of loops plus 1 (N + 1) required for the infinite series to meet the convergence criteria (LOOPS), the last value of m_k for each x iteration (M(k)), an interim coefficient value (COEF2), the coefficients of the $\cos(m_0|x-a| - \sigma t)$ term in Equation [2] (PHI1), and the coefficient of the $\sin \sigma t$ term in Equation [B-4] (PHI2A(k)).

The execution time for the program is in the neighborhood of 10 sec for the sample problem. The greatest amount of time is consumed in determining the convergence value of PHI2(k) for the $x = a = 0$ case. The program is quite economical to operate.

PROGRAM LISTING

```

PROGRAM FINDEP(INPUT,OUTPUT,TAPE5=INPUT,TAPE6=OUTPUT)
DIMENSION PHI2(200),X(200),Y(200),PHI1(200),ETA(200),NO(200),ARG(2
100),ARGH(200),PMU(200),BMU(200),WAYOUT(200),COEF2(200),PHIMA(100),
2PHI2A(100)
REAL LAMBDA
INTEGER STOPZ
COSH(W)=0.5*(EXP(W)+1.0/EXP(W))
SINH(W)=0.5*(EXP(W)-1.0/EXP(W))
READ(5,1) Q,G,F,H,A,B,T
1 FORMAT(7F10.4)
READ(5,2) STEPX,STEPY,STOPZ
2 FORMAT(2F10.4,I6)
SIGMA=F*F/G
SIGMA2=SIGMA*SIGMA
SIGMAH=SIGMA*H
CALL ROOT1(SIGMAH,FMU,N)
GMU=FMU/H
LAMBDA=6.2832/GMU
GMU2=GMU*GMU
FREQ=F*T
POWA=EXP(-FMU)
AMPLI=Q*F/G
COSF=COS(FREQ)
SINF=SIN(FREQ)
ANGL1=COSH(GMU*(B+H))
ANGL2=SINH(2.*FMU)
ANGL3=COSH(FMU)
COEF1A=(GMU+SIGMA)*POWA*ANGL3/GMU
COEF1B=ANGL1/(2.*FMU+ANGL2)
COEF1=2.*COEF1A*COEF1B
X(1)=-STEPX
Y(1)=-STEPY
DO 100 JJ=2,STOPZ
X(JJ)=X(JJ-1)+STEPX
Y(JJ)=Y(JJ-1)+STEPY
ARG(JJ)=GMU*(ABS(X(JJ)-A))-FREQ
ARGH(JJ)=GMU*(Y(JJ)+H)
PHI1(JJ)=COEF1*COSH(ARGH(JJ))
PHI2(1)=0.
COEF2(1)=0.
KK=0
KMIN=0
KMAX=0
DO 90 K=2,190
L=K
CALL ROOT2(SIGMAH,AMU,I,K)
IF(I.GT.100) GOTO 50
BMU(K)=AMU
AMU=AMU/H

```

```

ARGO=AMU*(Y(JJ)+H)
ARG1=AMU*(R+H)
POW=AMU*ABS(X(JJ)-A)
AMU2=AMU*AMU
COEF2(K)=(AMU2+SIGMA2)/(AMU*(H*AMU2+H*SIGMA2-SIGMA))
IF(POW.GE.200.0) GO TO 56
PHI2(K)=PHI2(K-1)*COEF2(K)*COS(ARG1)*COS(ARGO)*EXP(-POW)
GO TO 57
56 PMIN=PHI2(K-1)
   PMAX=PHI2(K-1)
   GO TO 43
57 IF(K.GT.4) GO TO 40
   GO TO 90
40 IF(PHI2(K-2).EQ.PHI2(K-1).AND.PHI2(K-1).EQ.PHI2(K)) GO TO 39
   IF(PHI2(K-2).GE.PHI2(K-1).AND.PHI2(K-1).LE.PHI2(K)) GO TO 41
   IF(PHI2(K-2).LE.PHI2(K-1).AND.PHI2(K-1).GE.PHI2(K)) GO TO 42
   GO TO 90
41 KMIN=KMIN+1
   PMIN=PHI2(K-1)
   IF(KMAX.EQ.0) GO TO 90
   GO TO 43
42 KMAX=KMAX+1
   PMAX=PHI2(K-1)
   IF(KMIN.EQ.0) GO TO 90
   GO TO 43
39 PMIN=PHI2(K-1)
   PMAX=PHI2(K-1)
43 KK=KK+1
   PMIMA(KK)=.5*(PMIN+PMAX)

22 IF(KK.GE.2) GO TO 44
   GO TO 90
44 DIFF=PMIMA(KK)-PMIMA(KK-1)
   IF(ABS(DIFF).LE..0001) GO TO 95
90 CONTINUE
95 NO(JJ)=L
   PHI2(NO(JJ))=PMIMA(KK)
   ETA(JJ)=AMPLI*(PHI1(JJ)*COS(ARG(JJ))-PHI2(NO(JJ))*SINF)
   PMU(JJ)=AMU
   WAYOUT(JJ)=COEF2(L)
   PHI2A(JJ)=PMIMA(KK)

```

```

100 CONTINUE
    GO TO 30
50 WRITE(6,55) I
55 FORMAT(20X,3H I=,I6)
    WRITE(6,58) JJ,K
58 FORMAT(20X,4H JJ=,I3//20X,3H K=,I3)
    GO TO 20
30 WRITE(6,7)
    WRITE(6,3)
3  FORMAT(110H PROGRAM TO COMPUTE THE FREE SURFACE DISTURBANCE DUE T
1  A STATIONARY PULSATING SOURCE IN WATER OF FINITE DEPTH)
    WRITE(6,4)
4  FORMAT(///// )
    WRITE(6,5)
5  FORMAT(22H THE INPUT VALUES ARE-)
    WRITE(6,6) Q,G,F,H,A,R,T
6  FORMAT(23X,17H SOURCE STRENGTH=,F10.4//23X,22H GRAVITATION CONSTAN
1T=,F10.4//23X,21H PULSATING FREQUENCY=,F10.4//23X,13H WATER DEPTH=
2,F10.4//23X,22H X LOCATION OF SOURCE=,F10.4//23X,22H Y LOCATION OF
3 SOURCE=,F10.4//23X,6H TIME=,F10.4)
    WRITE(6,11) STEPX,STEPY,STOPZ
11 FORMAT(//23X,7H STEPX=,F10.4//23X,7H STEPY=,F10.4//23X,7H STOPZ=,I
13)
    WRITE(6,7)
7  FORMAT(1H1)
    WRITE(6,12) SIGMA,GMU,ANGL1,SINF,COEF1,COEF1A,COEF1B
12 FORMAT(7H SIGMA=,F10.4/5H GMU=,F10.6/7H ANGL1=,F10.2/6H SINF=,F10.
16/7H COEF1=,F10.4/8H COEF1A=,F10.4/8H COEF1B=,F10.4)
    WRITE(6,8) LAMBDA
8  FORMAT(18H THE WAVELENGTH IS,1X,F10.4)
    WRITE(6,4)
    WRITE(6,9)
9  FORMAT(5X,2H X,10X,2H Y,11X,12H WAVE HEIGHT,4X,6H LOOPS,8X,5H M(K)
1,10X,6H COEF2,9X,5H PHI1,9X,9H PHI2A(K))
    WRITE(6,10) (X(II),Y(II),ETA(II),NO(II),PMU(II),WAYOUT(II),PHI1(II)
1,PHI2A(II),II=2,STOPZ)
10 FORMAT(1X,F10.4,2X,F10.4,7X,F10.5,8X,I3,5X,F10.4,5X,F10.4,5X,F10.4
1,6X,F10.6)
20 STOP
    END

```

```

SUBROUTINE ROOT1(SIGMAH,FMU,N)
N=0
3 IF(SIGMAH-.7) 10,10,4
4 IF(SIGMAH-1.0) 13,60,5
5 IF(SIGMAH-1.2) 15,15,6
6 FMU=SIGMAH
7 GO TO 21
10 D=.5*SQRT(9.-12.*SIGMAH)
FMU=SQRT(1.5-D)
GO TO 21
13 FMU=1.19
GO TO 21
15 FMU=1.2
21 N=N+1
A=FMU*(TANH(FMU))-SIGMAH
B=FMU*(1.0-TANH(FMU)*TANH(FMU))+TANH(FMU)
C=ABS(A/B)
IF((C/FMU)-.00001) 50,50,30
30 IF(N-100) 40,50,50
40 FMU=FMU-A/R
GO TO 21
50 RETURN
60 FMU=1.19967
RETURN
END
C SUBROUTINE TO COMPUTR THE REAL, POSITIVE ROOTS OF THE EQUATION
C (M)*TAN(M)+P=0
SUBROUTINE ROOT2(SIGMAH,AMU,I,K)
C TESTS TO SET AN INITIAL VALUE FOR AMU
IF (K-2) 4,4,5
4 AMU=((SIGMAH+.01)/SIGMAH)*3.1416/2.
GO TO 8
5 G=K
AMU=((SIGMAH+.01)/SIGMAH)*3.1416/2.+(G-2.0)*3.1416
GO TO 8
C START OF THE NEWTON-RAPHSON ITERATION
8 I=0
9 I=I+1
T=AMU*TAN(AMU)+SIGMAH
B=AMU*(1.0+TAN(AMU)*TAN(AMU))+TAN(AMU)
R=ABS(T/B)
C TEST FOR SIZE OF INCREMENTAL ESTIMATE
IF(R.LE..00001) RETURN
IF(I.GT.100) RETURN
AMU=AMU-T/R
GO TO 9
END

```

Sample Output

PROGRAM TO COMPUTE THE FREE SURFACE DISTURBANCE DUE TO A STATIONARY PULSATING SOURCE IN WATER OF FINITE DEPTH

THE INPUT VALUES ARE-

```

SOURCE STRENGTH= 1.0000
GRAVITATION CONSTANT= 32.2000
PULSATING FREQUENCY= 3.5000
WATER DEPTH= 6.0000
X LOCATION OF SOURCE= 0.0000
Y LOCATION OF SOURCE= -4.0000
TIME= 2.0196

STEPX= 1.0000
STEPLY= 0.0000
STOPZ= 42
    
```

```

SIGMA= .3804
GMU= .387757
ANGL1= 1.32
SINF= .707114
COEF1= .0461
COEF1A= 1.0000
COEF1B= .0230
THE WAVELENGTH IS 16.2040
    
```

X	Y	WAVE HEIGHT	LOOPS	MIK1	COEF2	PHI1	PHI2A(K)
0.0000	0.0000	.03921	52	26.7012	.0062	.2383	-.271801
1.0000	0.0000	-.03839	13	6.2731	.0266	.2383	-.188727
2.0000	0.0000	.03567	10	4.6989	.0356	.2383	-.127040
3.0000	0.0000	-.03058	8	3.6679	.0459	.2383	-.084455
4.0000	0.0000	.02301	8	3.6679	.0459	.2383	-.056399
5.0000	0.0000	-.01340	8	3.6679	.0459	.2383	-.037678
6.0000	0.0000	.00271	8	3.6679	.0459	.2383	-.025237
7.0000	0.0000	-.00778	8	3.6679	.0459	.2383	-.016936
8.0000	0.0000	-.01670	8	3.6679	.0459	.2383	-.011379
9.0000	0.0000	-.02288	8	3.6679	.0459	.2383	-.007651
10.0000	0.0000	-.02548	8	3.6679	.0459	.2383	-.005146
11.0000	0.0000	-.02417	8	3.6679	.0459	.2383	-.003462
12.0000	0.0000	-.01919	8	3.6679	.0459	.2383	-.002329
13.0000	0.0000	-.01131	8	3.6679	.0459	.2383	-.001568
14.0000	0.0000	-.00171	7	3.1214	.0537	.2383	-.001055
15.0000	0.0000	.00817	7	3.1214	.0537	.2383	-.000710
16.0000	0.0000	.01685	7	3.1214	.0537	.2383	-.000478
17.0000	0.0000	.02304	7	3.1214	.0537	.2383	-.000321
18.0000	0.0000	.02582	7	3.1214	.0537	.2383	-.000216
19.0000	0.0000	.02477	7	3.1214	.0537	.2383	-.000146
20.0000	0.0000	.02004	7	3.1214	.0537	.2383	-.000098
21.0000	0.0000	.01234	7	3.1214	.0537	.2383	-.000066
22.0000	0.0000	.00281	7	3.1214	.0537	.2383	-.000044
23.0000	0.0000	-.00713	7	3.1214	.0537	.2383	-.000030
24.0000	0.0000	-.01602	7	3.1214	.0537	.2383	-.000020
25.0000	0.0000	-.02253	7	3.1214	.0537	.2383	-.000014
26.0000	0.0000	-.02569	7	3.1214	.0537	.2383	-.000009
27.0000	0.0000	-.02504	7	3.1214	.0537	.2383	-.000006
28.0000	0.0000	-.02067	7	3.1214	.0537	.2383	-.000004
29.0000	0.0000	-.01323	7	3.1214	.0537	.2383	-.000003
30.0000	0.0000	-.00383	7	3.1214	.0537	.2383	-.000002
31.0000	0.0000	.00614	7	3.1214	.0537	.2383	-.000001
32.0000	0.0000	.01520	7	3.1214	.0537	.2383	-.000001
33.0000	0.0000	.02201	7	3.1214	.0537	.2383	-.000001
34.0000	0.0000	.02554	7	3.1214	.0537	.2383	-.000000
35.0000	0.0000	.02528	7	3.1214	.0537	.2383	-.000000
36.0000	0.0000	.02127	7	3.1214	.0537	.2383	-.000000
37.0000	0.0000	.01410	7	3.1214	.0537	.2383	-.000000
38.0000	0.0000	.00484	7	3.1214	.0537	.2383	-.000000
39.0000	0.0000	-.00515	7	3.1214	.0537	.2383	-.000000
40.0000	0.0000	-.01436	7	3.1214	.0537	.2383	-.000000